I.J. Wireless and Microwave Technologies, **2025, 1, 40-50**
Published Online on February 8, 2025 by MECS Press (http://www.mecs-press.org/)
DOI: 10.5815/ijwmt.2025.01.03

Metamaterial Inspired Millimeter-Wave Antenna Arrays for 5G Wireless Applications

Moti G. Beyene*
Jimma Institute of Technology /Electrical and Computer Engineering, Jimma, Ethiopia
E-mail: motibyenegole@gmail.com
ORCID iD: https://orcid.org/0009-0005-2073-4671
*Corresponding Author

Isayiyas T. Nigatu
Jimma Institute of Technology /Electrical and Computer Engineering, Jimma, Ethiopia
E-mail: isayiyas.tiba@ju.edu.et
ORCID iD: https://orcid.org/0000-0002-0606-2558

Received: 28 June, 2024; Revised: 15 August, 2024; Accepted: 12 September, 2024; Published: 08 February, 2025

Abstract: Fifth-generation (5G) wireless communication systems employ millimeter-wave (mm-wave) frequency bands to achieve a very broad spectrum for high data rate transmission. To meet the system requirements, the best design of antenna arrays with superior performance is essential. Thus, in this paper, the design and performance analysis of single element, 2 x 1, and 4 x 1 metamaterial inspired millimeter-wave antenna (MIA) arrays are proposed. The antenna elements are designed using Rogers' 5880 as a substrate material with a 2.2 dielectric constant and thickness of 0.35 mm to operate at a center frequency of 38 GHz. The simulated design of the single, 2 x 1, and 4 x 1 MIA arrays return loss, bandwidth, gain, voltage standing wave ratio (VSWR), and total efficiency are: -82.95 dB, -67.1 dB, -69.12 dB; 1.971 GHz, 2.278 GHz, 4.704 GHz; 7.36 dBi, 9.11 dBi, 11.4 dBi; 1.001432, 1.0009, 1.0007; and 95.55 %, 94.01 %, 95.87. As compared to other works, improved performance has been achieved by considering the effect of meta-materials on the radiator and at the ground of microstrip patch antennas (MPA). The selected type of meta-materials alters the current distribution of the radiating patch that enhances the fringing fields at the edge of MPAs, which inspires the radiation of antennas and reduces the surface wave loss at the radiators' ground plane. The proposed MIA antenna arrays have improved upon the drawbacks of traditional MPAs and fulfill the requirements of 5G communication systems.

Index Terms: Bandwidth, Beam-Gain, Directivity, Meta-material, Split Ring Resonator (SRR), Return loss

1. Introduction

The 5G communication systems are transforming telecommunication applications by using spectra such as sub-6 GHz, 24 GHz, 28 GHz, and 38 GHz. These frequencies were chosen because of their wide bandwidth (BW) availability, higher throughput, and low latency, which will enable several new wireless applications [1]. Compact radiating antennas capable of operating over wide frequency bands should be designed to make such promises a reality. Recently, an MPA with miniaturized technology through a negative-permittivity dielectric substrate has been proposed to meet these requirements [6]. Shorting walls, shorting pins, some deformation, and fractal geometry are used in the MPA. However, the overall performance of such an approach is limited since the BW is narrow, the magnitude of the return loss is very high [14], and the radiation efficiency is also minimal due to surface and spurious wave losses and dielectric losses of MPAs [2]. As such, an alternative design approach based on the use of meta-materials is proposed to address these issues. In [3, 4, 5], the SRR structures are used as radiators, while in [6, 7] they are used on the ground of the antennas. Further, the work in [8] also reported the usage of SRR structures as a super-state of the designed antennas. Besides, a compact meta-material [9] and ultra-wide-band planar arrays [10] are designed from a slot of SRR structures as the main resonator and a co-planar wave-guide at the feeding part. Similarly, an mm-wave meta-material SRR loaded that operated at 28 GHz is presented in [11] to enhance the BW of meta-materials using the structure of an SRR on the substrate layer. The above works are commonly considered SRR structure-based antenna designs and are able to improve certain parameters. However, there are several issues that need to be addressed to be able to design compact radiating antennas that can meet the requirements of 5G and beyond mobile networks. On one hand, the designed

This work is open access and licensed under the Creative Commons CC BY 4.0 License.

antennas in the existing works have no common resonant frequency, and the antenna has cross-polarization, causing array blindness and low BW. Besides, the interaction between the SRR structures and an antenna was not investigated, even though it is crucial for the current distribution, which profoundly determines the antenna performance

To address these issues, in this work, a design of MIA array that resonates at 38 GHz was proposed. The aim is to design a high overall performance antenna by exploiting the artificial properties of SRR structures with compact antenna sizes. A step-by-step, design process of the radiator is considered to identify the impact of SRR structures on propagation scenarios. Further, the properties of the slotted structures have been studied to overcome challenges with design complexity issues and operate at a higher frequency. The rest of this paper is organized as follows: Section 2 describes the design of the proposed antenna. Section 3 presents the simulation analysis and discussion, and, section 4 concludes this work.

2. Design of Metamaterial Inspired Millimeter-Wave Antenna Arrays

This section provides the design steps for the proposed MIA arrays for the 5G communication systems at 38 GHz. First, the design steps in the conventional microstrip patch antenna were introduced and then present the design procedure of the proposed MIA arrays along with a detail discussion about its operation.

2.1. Designing steps

Initially, the design steps detailed in [20] was used to create a single-element conventional MPA physical structure as an initial model. To use a substrate of low dielectric loss, better mechanical energy and suited for high frequencies, the RT Rogger's 5880 was selected [20]. These properties make it well-suited for high-frequency and high-power applications, including 5G systems. Figure 1 depicts the front view of the rectangular MPA. As discussed in the preceding section, the performance of such a structure is constrained by a number of losses. For instance, in order to achieve a wide bandwidth, the substrate thickness in an MPA system must be sufficiently large. However, as the substrate thickness increases, surface and spurious wave losses occur, resulting in limited performance.

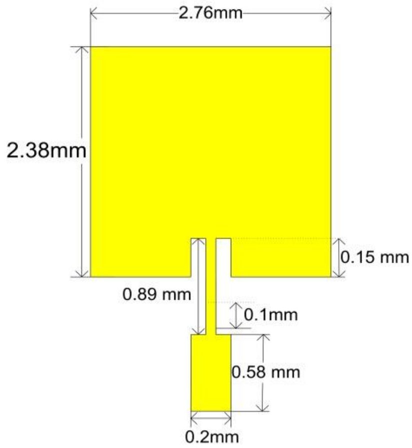

Fig. 1. Typical Rectangular MPA.

Table 1. Calculated Dimensions of Typical Rectangular MPA.

Antenna Component	Symbol	Calculated Dimensions (mm)	Optimized Dimensions (mm)
Ground Width	W	5.72	5.72
Ground Length	L	5.22	5.22
Patch Width	Pw	3.12	2.76
Patch Length	Lpl	2.437	2.38
Copper Thickness	Cu	0.035	0.035
Substrate Thickness	H	0.35	0.35
Permittivity	ϵr	2.2	2.2
Inset feed	f*gp*	0.2656	0.15

Table 2. Calculated Dimensions of Typical Rectangular MPA.

SRR Component	Symbol	Calculated Dimensions (mm)	Optimized Dimensions (mm)
Outer Length	Lo	0.96	0.5
Inner Length	Li	0.52	0.3
Gap	Rgp	0.13	0.05
Thickness	Rthick	0.15	0.05
Gap Between Rectangle	Cu	0.09	0.1

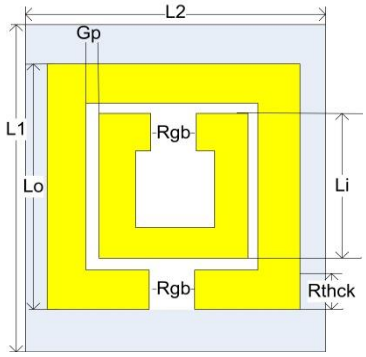

Fig. 2. Meta-material SRR Structure Slot.

2.2. To reduce different types of losses and improve antenna performances the following steps are followed.

1. A new structure by integrating SRR structure slots into the conventional radiator and the ground plane was presented. In this approach, since the properties of electric and magnetic fields are used to select SRR structures, changing these fields can cause the MPA's characteristics to change in such a way that performance can be improved without increasing the physical size or the losses.
2. By inspiring these new ideas, a developed slot of basic SRR structure shown in Fig. 2 is designed. As illustrated in this figure, there is an air gap between the outer and inner rings of SRR, resulting in different resonant frequencies.
3. To determine the frequencies and the physical dimensions of the proposed SRR structures, the following procedure has been employed: Suppose that L denotes the length and Lo, Li are the outer and inner lengths, respectively. Then the lengths $L1$, $L2$ can be calculated using equation 1 and 2 [21, 22], respectively.

$$\mathrm{L1} = 4(\mathrm{Lo} - \mathrm{Rthck}) - \mathrm{Rgp} \tag{1}$$

$$\mathrm{L2} = 4(\mathrm{Li} - \mathrm{Rthck}) - \mathrm{Rgp}, \tag{2}$$

Here R_{thck}, R_{gp} denote the thickness of the rectangle, and the gap, respectively. Further, the inner-outer frequencies f_{outer} , f_{inner} can be computed as

$$f_{\mathrm{outer}} = \frac{c}{2L_1\sqrt{\epsilon_{\mathrm{eff}}}} \tag{3}$$

$$f_{\mathrm{inner}} = \frac{c}{2L_2\sqrt{\epsilon_{\mathrm{eff}}}} \tag{4}$$

Respectively, where C denotes the speed of light $(\approx 3.0 \times 10^8 \text{ m/s})$. The ϵ_{eff} is computed as

$$\epsilon_{\mathrm{eff}} = \frac{\varepsilon_r+1}{2} + \frac{\varepsilon_r-1}{2\sqrt{1+12\frac{h}{Lo}}} \tag{5}$$

Where ε_r is permittivity and h denotes the substrate thickness. When two resonators with two different resonant frequencies f_{outer} and f_{inner} are coupled, the coupling changes both resonances by f_o. The frequency variation depends on the coupling values between the two rings and the resonant frequency of each loop occurs at halfwavelength, which can be determined as:

$$f_{\mathrm{o}} = \frac{c}{2L_{\mathrm{eq}}\sqrt{\epsilon_r}} \tag{6}$$

Where $L_{\mathrm{eq}} = \frac{L_1+L_2}{2}$.

4. As such, the SRR structure slot designed with the above equation was implemented on both the ground and radiator parts of the antennas. This leads to low loss properties by reducing the return loss, impedance mismatching, and other losses, such as surface wave and spurious wave losses.

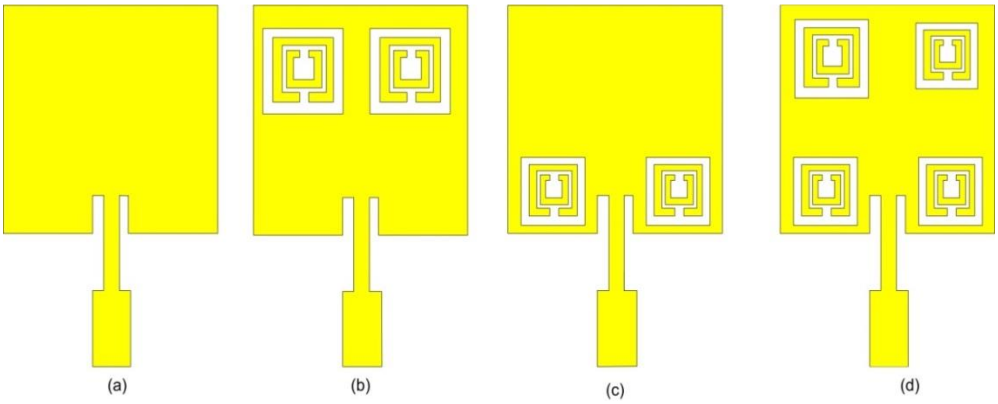

Fig. 3. Design steps of single element MIA arrays

5. Figs. 3(a)-(d) depict the design steps for a single-element MIA. In this structure, the SRR structure slot placement is technically selected to reduce the drawbacks of a typical rectangular MPA.
6. As it can be seen from the figure, the SRR structure slot is introduced on the upper and lower parts of the radiator in this way, it affects the antenna performance.
7. More specifically, the introduced SRR structure slot in Fig. 3(b) is used to alter and then enhance the magnitude of the fringing fields from the radiator to the atmosphere.
8. Next, the structure in Fig. 3(c) is developed to minimize the returned power to the source and regulate the flow and path current distribution at the feeding edge of MPAs.
9. Finally, an MIA antenna that can achieve improved performance is constructed by integrating the structures from the previous steps, as shown in Fig. 3(d). Based on the above instructive idea, our proposed design of the MIA antenna is shown in Fig. 4.

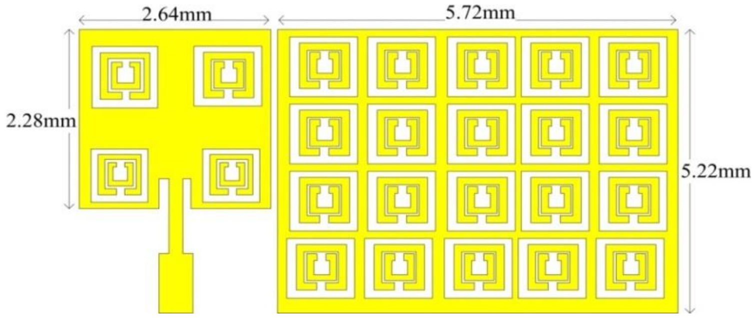

Fig. 4. Single element metamaterial inspired mm-wave antenna arrays.

This figure depicts the front view of the rectangular MPA inspired by 2 x 2 and 4 x 5 meta-material SRR slot arrays on the ground structure. The metamaterial SRR slot has been placed at a distance of 1 mm from each other to reduce mutual coupling between antenna elements. As a summary of the designing steps, the physical structure of the designed MIA arrays along with the dimensions are indicated in Figs. 5-6.

2.3. Why SRR works

In this subsection, we present the reasons why the proposed MIA design can achieve improved performance at large frequencies such as 38 GHz. Adjusting the split gap used the SRR act as a resonant circuit that provides a low-impedance path for the surface currents on the patch antenna, effectively shorting out the currents at the edges of the patch. Couple with the patch and create new resonant modes that expand the operating bandwidth of the antenna and re-radiate the energy that is otherwise lost in the substrate. It can suppress the surface wave propagation on the patch antenna and improve the antenna’s isolation. Also, the SRR slot reduces the cross-polarization to improve polarization purity and mitigate the level of unwanted signals. This can make the designed antennas more compact and reduce its profile, making it easier to integrate into a smaller device. The performance of MPA is significantly impacted by the magnitude of the fringing fields. Fig. 7 demonstrates the impacts of a meta-material SRR inspired on the fringing area of an MPA. Because of the SRR slots, the circled flow of the current at the head of SRR rings are dismissed and charges stored at the edge of the ring accepts the capacitance behavior. As the capacitance value gathered by the edge of SRR slot increased, the antenna and source impedance will be matched. The arranged array SRRs that inserted at the ground of the radiator will store more charges and the spurious wave mitigated to improve power capacity and bandwidths.

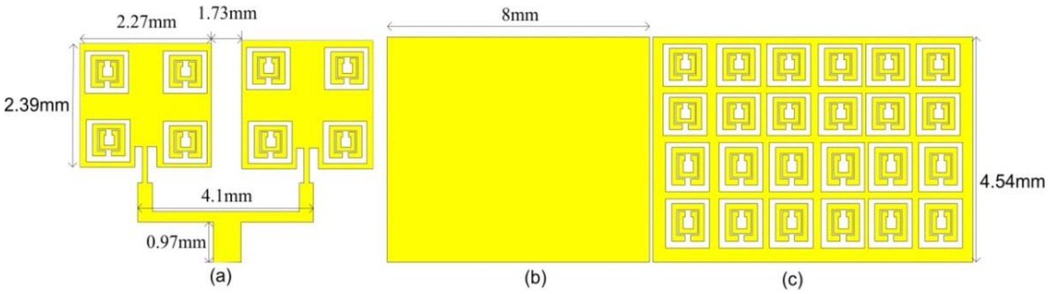

Fig. 5. 2 x 1 metamaterial inspired mm-wave antenna arrays (a), Without (b) and with 6 x 4 SRRs (c).

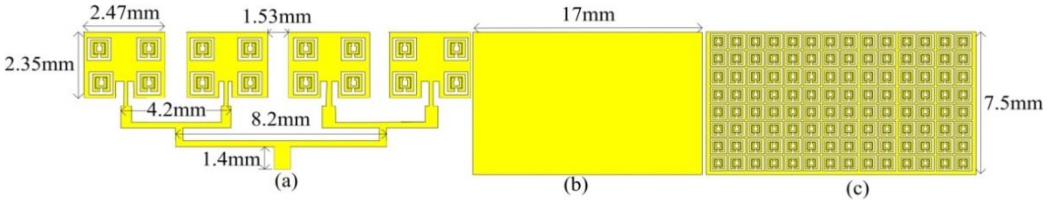

Fig. 6. 4 x 1 metamaterial inspired mm-wave antenna arrays (a), Without (b) and with 16 x 7 SRRs (c).

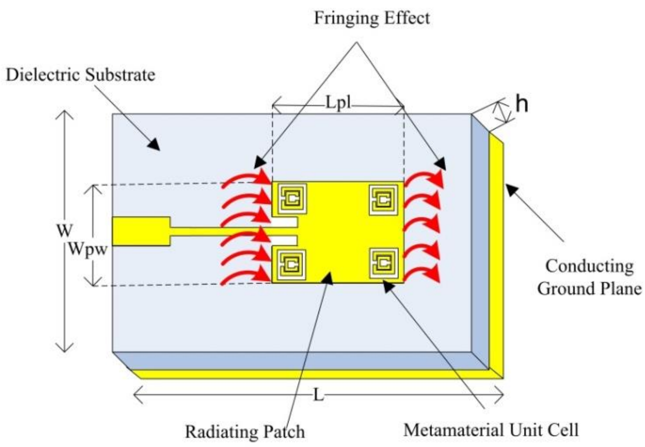

Fig. 7. Effect of Meta-material SRR structure inspired on the fringing area of MPA.

While the current is induced by an electric field between the gaps of SRR metal, the side length acts as an inductance. The inductive properties of this metallic ring produce magnetic fields by reducing the loss current of the radiator which will affect the impedance and bandwidths of the proposed antennas. So, this principle of the proposed SRR slot increases the radiation capacity of the proposed antenna. To regulate and match the proposed antennas impedance at the feeding network, the split gap, side lengths, and the width of the SRR has been analyzed. Since there is no fringing of electric fields along the length of the radiating patch, the radiation caused by the fringing field that occurred between the MPA’s edge and the ground plane (along the width of the patch) would be used for communication purposes. Furthermore, the magnitude of the fringing field is affected by the MPA size and substrate height. Technically, the fringing field gets larger as the height of the substrate increases. A MPA would appear electrically broader in comparison to its physical part due to the fringing effect. Thus, it is necessary to increase the fringing effect of MPAs to attain antennas with good performance for efficient radio propagation, and the meta-materials have a great role in increasing the fringing effects. As shown in Fig. 4, the meta-material SRR structure inspired applied to the patch. This decreases the high input impedance of typical MPA and changes the current distribution pattern, which profoundly boosts the magnitude of the current arriving at the center and the edge of the radiating patch. This helps the MPA radiate the input power strongly and increase the effective length. In another perspective, the meta-materials SRR structure added at the ground of the antennas are desired to act as a reflecting surface, which will focus the maximum radiation energy in the desired direction. Also, it suppresses the surface wave loss of the antenna; hence, the returned loss and VSWR are highly improved. As such, employing the proposed method at the effective fringing area allows us to improve antenna performance metrics such as bandwidth, gain, directivity, and radiation efficiency.

3. Simulation Results and Discussions

In this section, the performance analysis of the proposed metamaterial-inspired millimeter-wave antenna arrays is presented based on time domain based simulations obtained from the CST-MW studio. The performance has been measured in terms of the bandwidth, magnitude of the return loss, VSWR, gain, and radiation efficiency. We begin the discussion by presenting the S-parameters, permittivity and permeability characteristics of the designed meta-material loaded in Fig. 2. Fig.8 (a) shows the real and imaginary reflection (S11) and transmission (S21) coefficient of the SRR slot.

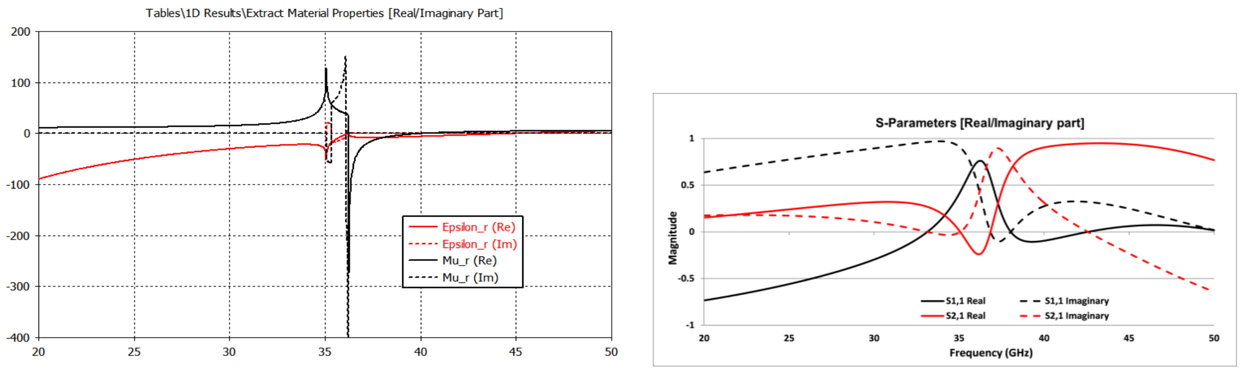

(a) S-parameters (Real and imaginary parts). (b) Permittivity and Permeability.

Fig. 8. Material properties of Meta-material SRR structure slot.

Material properties of the SRR slot are extracted from S-parameters. From the simulated result depicted in Fig. 8 (b), it is clear that the magnitude of the plot is within the negative and positive regions for permittivity and permeability, respectively. At the proposed resonant frequencies, SRR structure slot permittivity and permeability are negative. This helps to know refractive index of SRR structure slot to design the reduced size and more performed antennas. In conventional scenarios, this plot characteristic is not obtained or exists. Thus, the designed SRR slot exhibits permittivity and permeability characteristics, which play a vital role in enhancing the antenna performance metrics. The real parts of Fig. 8 (b) represent the ability to store electric and magnetic energy, and the imaginary part of permittivity and permeability appeared by the sake of the loss in electric and magnetic energies. As shown in Fig. 8 (b) the negative permeability of the SRR structure slot is from 36.2GHz to 40.17GHz and negative permittivity up to 45.12GHz. The proposed SRR slot will appear double negative with a bandwidth of 3.97GHz to satisfy the characteristics of DNG meta-materials.

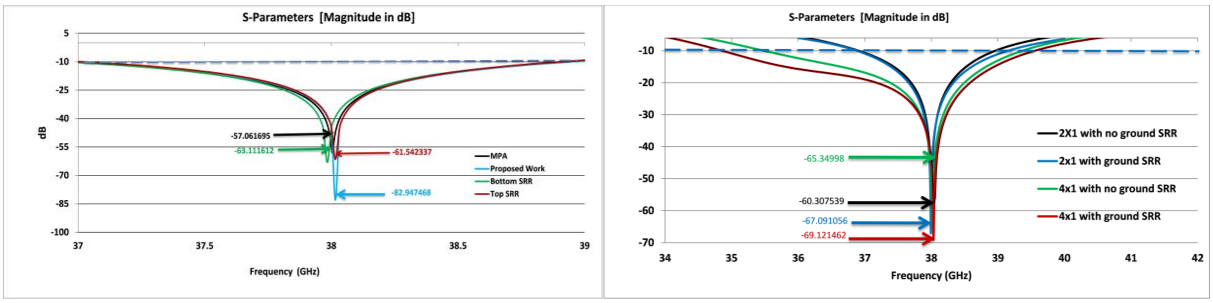

(a) Single Typical MPA and MIA . (b) 2 x 1 and 4 x 1 MIA arrays.

Fig. 9. Return loss Vs Frequency Plot of antennas.

The return loss versus frequency plot of a single rectangular MPA and MIAs is shown in Fig. 9 (a). As it can be seen from the plots, the conventional MPA has a return loss near -57 dB, while the proposed MIA antenna has been able to achieve below -82 dB at a BW of about 2.081 GHz. This shows that using a meta-material SRR structure slot as an antenna part and ground can significantly reduce return loss, with our method being able to reduce it by less than -25 dB. Furthermore, when we compare the results corresponding to the MIA arrays, it is clear that the bottom and top metamaterial SRR structure-inspired antennas have a large return loss compared with 2 x 2 metamaterial SRR inspired. This is due to the fact that the top SRR slot is used to enhance the fringing fields of the patch, which results in reducing input power loss. Besides, using the bottom SRR slot changes propagation direction and, as a result, produces better radiation from the antenna. Our result confirms this fact by reducing the reflection coefficient up to -82.95 dB and matching the impedance of the antenna. Fig. 9 (b) plots the return losses of 2 x 1 and 4 x 1 MIA arrays. It is clear from the figure that the 2 x 1 and 4 x 1 MIA arrays have achieved return losses of -60.3 dB and -67.1 dB, respectively, both without and with incorporating a 6 x 4 MIA arrays on the ground plane. Besides, it can be easily seen that, as MIA arrays are integrated into the structure, the bandwidth of the 2 x 1 MIA arrays is changed from 2.057 GHz to 2.278 GHz, which shows an improvement of 221 MHz. Furthermore, it is also clear that the 4 x 1 MIA arrays return losses without and with SRR slots on the ground are -65.35 dB and -69.12 dB, respectively. The antenna's BW was approximately 3.89 GHz prior to the use of meta-materials; after the use of meta-materials, however, it is increased to 4.704 GHz. As such, it is clear from the results, that, by arranging the flow of current to the center of the patch and decreasing the impedance, the inserted meta-materials at the edge of each MPA attenuate the circulation current which causes large magnitude of the return losses. Figs. 10(a)-(b) show comparisons of VSWR for single-element MPA and MIA arrays and those of 2 x 1 and 4 x 1 antenna arrays, respectively.

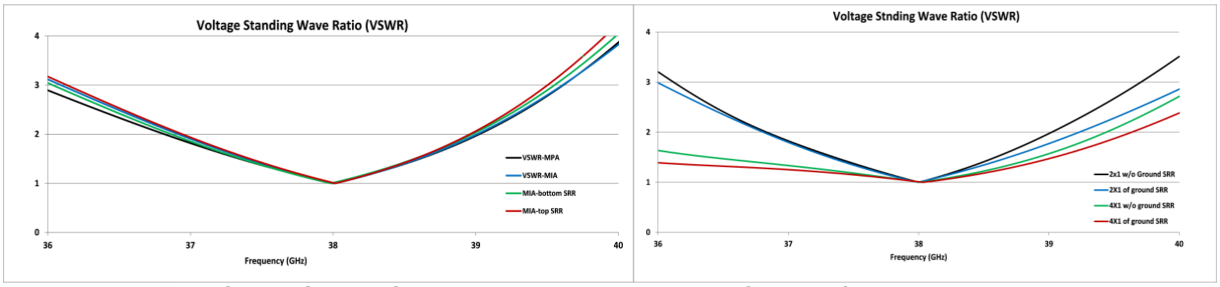

(a) Single Typical MPA and MIA. (b) 2 x 1 and 4 x 1 MIA arrays.

Fig. 10. VSWR plots of MPA and MIA arrays.

The VSWR of conventional and MIA single elements is 1.0181 and 1.0014, respectively. Similarly, the VSWR of 2 x 1 and 4 x 1 without SRR slots on the ground of antennas is 1.0019 and 1.0002, respectively. The VSWRs of the proposed 2 x 1 and 4 x 1 MPAs with SRR slots, on the other hand, are 1.0009 and 1.0007, respectively. From the results, it can be observed that the introduced MIA arrays at the side of the feed line (i.e., the bottom SRR slots) reduces the mismatch loss of the antenna and can be considered an effective way to minimize the mismatch loss of conventional microstrip antennas. The 2D radiation pattern of a typical single-element Microstrip patch antenna, MIA of single element, 2 x 1, and 4 x 1 arrays are given in Figs. 11(a)-(b). 11(a) shows Fig a 2D radiation pathtern comparison between MPA and MIA. As it can be seen from the plot, the side lobe level magnitude of a conventional and modified single element patch antenna are -25.6 dB and -15.2 dB. As the SRR slot is introduced only on the radiating patch of 2 x 1 and 4 x 1 arrays, the achieved side lobe level is about -15.6 dB and -11.3 dB, respectively. At millimeter wave bands the wavelength of the signal is short.

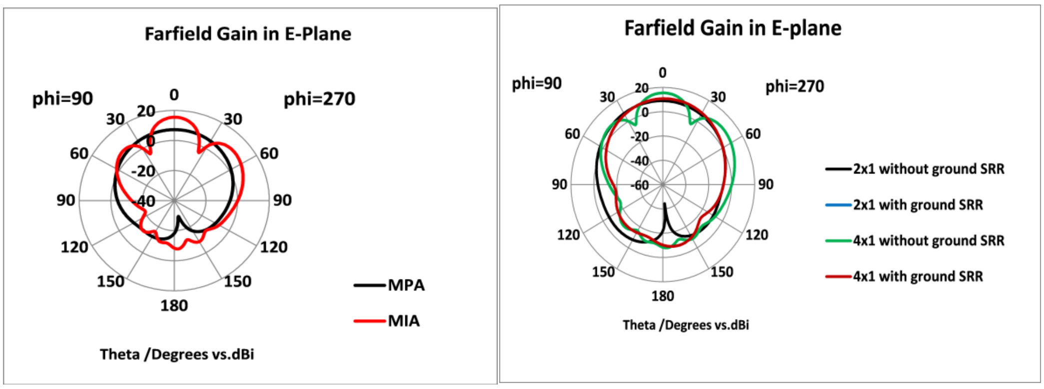

(a) (b)

Fig. 11.

This allows for more compact antenna designs, but also makes the antenna's performance more sensitive to factors like side lobe levels and radiation pattern control. Metamaterial inspired millimeter wave antennas operating at high frequencies can be designed to exploit the unique properties of metamaterials to achieve desirable radiation characteristics. In high frequency bands and closely spaced frequency channels, high side lobes can lead to adjacent channel interference and can distort the main beam of the antenna's radiation pattern. This distortion can reduce the precision of the beam, impacting the accuracy of applications like radar or beam forming systems. High-frequency bands like millimeter waves, high side lobes can lead to significant interference with neighboring cells or users. This interference can reduce network capacity and overall performance. To improve these scenarios MIA are analyzed and proposed. Likewise, as the SRR slot is integrated on the radiator and ground plane of the array simultaneously, the obtained side lobe level of 2 x 1 and 4 x 1 arrays are -13.6 dB, and -11.3 dB, respectively. From the results, it can be easily realized that, as the number of SRR slot arrays on the ground plane increases, the magnitude of the side lobe level increases which is loss of input power and produces the interference at the receiver side. Because, the SRR slot arrays reflect the radiated EM to undesired direction. However, deploying the SRR slots on the ground enhances the bandwidth of all the designed antennas.

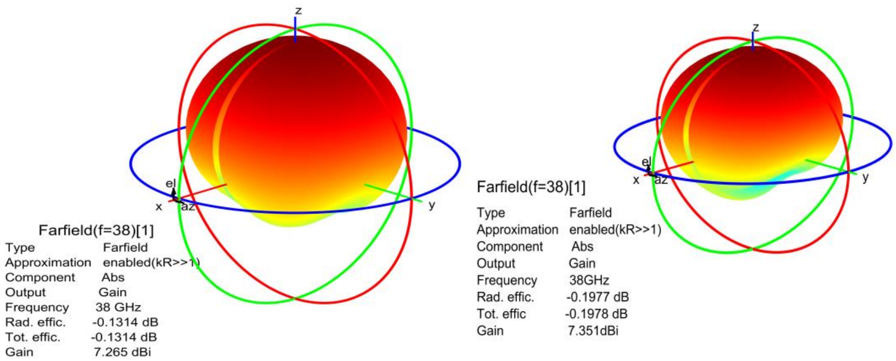

(a) Single MPA. (b) Single MIA.

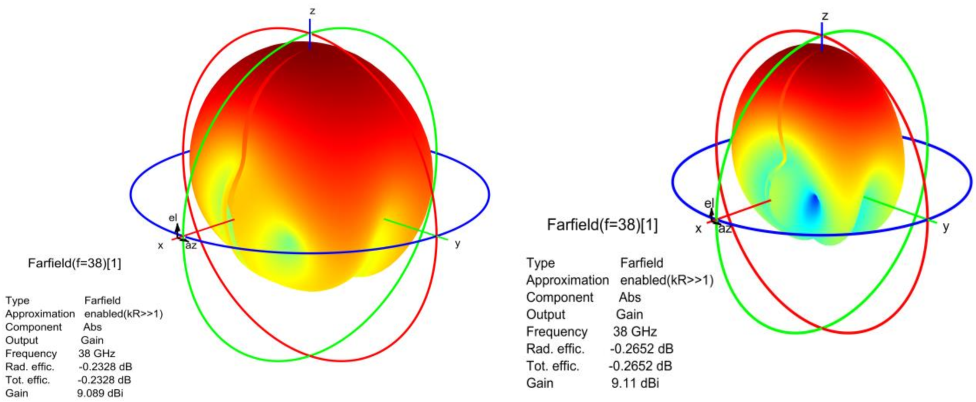

(c) 2 x 1 antenna without ground SRR slot array. (d) 2 x 1 antenna with ground 6 x 4 SRR slot array.

Fig. 12. 3D Radiation Pattern of Single Element and 2 x1 MIA arrays.

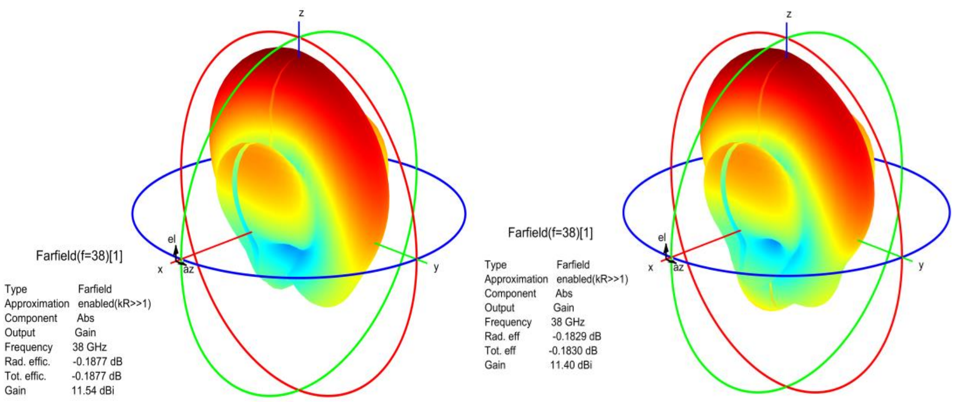

(a) 4 x 1 antenna without ground SRR slot array. (b) 4 x 1 antenna with ground 16 x 7 SRR slot array.

Fig. 13. 3D Radiation Pattern of 4 x 1 MIA arrays.

To further investigate the performance of the new design, Figs. 12(a)–(d) show a three-dimensional view of the radiation pattern. As it is clear from Figs. 12(a)-(b), the gain, radiation efficiency, and total efficiency corresponding to the conventional MPA and the proposed single-element MIA are 7.26 dBi, -0.1314, 97.02%, and 7.36 dBi, -0.1978, 95.55 %, respectively. Using the same pattern, the results in Figs. 12(c)-(d) shows that the gain, radiation efficiency, and total efficiency of a 2 x 1 MIA that is meta-material added on the patch and the 6 x 4 SRR slot arrays on the patch and ground of the antenna are 9.09 dBi, -0.2328, -0.2328 (94.78%), and 9.11, -0.2652, -0.2652 (94.01%), respectively. Figs 13(a)-(b) implies the introduced SRR slots only on the patch and then on both the radiator and ground of antennas, the achieved gain, radiation efficiency, and total radiation efficiency of 4 x 1 MIA arrays are about 11.5 dBi, 95.77%, and 11.4 dBi, 95.87%, respectively. The proposed work discusses by comparing the performance of the proposed antenna with several existing antenna designs. Table 3 lists the comparison in terms of various parameters. The proposed single MIA arrays has a very low return loss and enhanced efficiency as compared to the results reported in [13, 14, 15, 16], and wide bandwidth is achieved as compared to the work reported in [15, 16]. In terms of the magnitude of the return loss, VSWR, and total efficiency, the 2 x 1 and 4 x 1 MIA arrays have better performance as compared to [14, 17, 18, 19, 23], and [24]. The reason to achieve better performance is because of the negative refractive index properties of meta-materials, which minimizes the returned power to the source, increases the fringing effect, and increase the radiation efficiencies of the MIA. While the introduced SRR slots at the ground of the antenna enhance the bandwidth by reducing the surface wave loss.

Table 3. Performance Comparison of the Proposed Design with Other Similar Works

Antenna Type	Ref. no	RF (GHz)	BW (GHz)	S11 (dB)	VSWR	Gain (dBi)	η(%)
Single	[13]	38	2.146	-40.54	1.02	6.85	95.4
	[14]	38	-	-20.15	1.27	8	90.32
	[15]	38	1.27	-42.78	1.08	9.025	83.61
	[16]	38	1.47	-29.45	0.995	7.89	-
	This Work	38	1.971	-82.95	1.0014	7.36	95.55
2x1	[14]	38	3.651	-18.35	1.27	9.24	89.63
	[17]	38	1.06	-22.6	-	9.75	80
	[23]	28	--	-28.84	1.075	9.69	--
	[24]	28	1.65	-22.5	1.16	9.5	91.4
	This Work	38	2.278	-67.1	1.0009	9.11	94.01
4x1	[18]	38	3.33	-20.15	1.27	5.5	84
	[19]	38	1.48	-24.25	-	6.98	-
	This Work	38	4.704	-69.12	1.0007	11.4	95.87

In real-world 5G deployments, antennas are often exposed to varying environmental conditions, including temperature fluctuations. Designing antennas to withstand these conditions while maintaining performance is critical. At high power levels generate more heat, so designing for high power operation requires robust thermal management solutions. Ensuring that the antenna can handle high power without significant performance degradation is essential. Thermal effects can significantly impact the performance of metamaterial-inspired antennas, especially in high-frequency and high-power 5G applications. Key concerns include thermal expansion, changes in material properties, increased resistance, and performance degradation. Effective thermal management, careful material selection, and thorough testing are crucial to mitigate these effects and ensure reliable performance of the antenna system. Addressing these challenges helps maintain the desired performance and reliability of metamaterial-inspired antennas in demanding 5G environments. While metamaterials offer many benefits, their complex structures can be challenging to manufacture at scale. Ongoing work focuses on developing cost-effective and scalable fabrication techniques. The performance of metamaterial antennas can be influenced by the properties of the materials used. Seamlessly integrating metamaterial-inspired antennas with existing 5G infrastructure and technologies is an ongoing challenge. Ensuring compatibility and optimizing performance across diverse applications is key to widespread adoption. Developing new materials that offer better performance characteristics and disabilities are the future work of the proposed paper.

4. Conclusions

In this paper, wide-band single, 2 x 1 and 4 x 1 MIA arrays are designed and simulated. The simulated result reveals that the designed single-element MIA bandwidth, return loss, gain, and total efficiency are 1.97 GHz, -82.95 dB, 7.36 dBi, and 95.55 % respectively. The bandwidth, return loss, gain, and total efficiency of 2 x 1 and 4 x 1 MIA arrays are 2.279 GHz, -67.1 dB, 9.11 dBi and 94.01 % and 4.704 GHz, -69.12 dB, 11.4 dBi and 95.87 %, respectively. Likewise, the obtained bandwidth and radiation efficiency of the 4 x 1 MIA arrays are 4.704 GHz and 95.87 %, respectively. From the achieved results, it can be concluded that the bandwidth of the antenna is improved and the magnitude of the return loss has been minimized as the antenna is inspired by meta-materials on both the radiating patch and ground structures. Besides, as the number of SRR slots increases at the ground of the antennas, the surface wave loss is decreased but the side lobe level is increased. The proposed design enables the design of compact antennas with high performance. This is particularly important for 5G devices, which are often designed to be smaller and more integrated and can achieve higher gain and directivity compared to conventional designs. This means they can focus energy more effectively, improving signal strength and coverage. Higher directivity also reduces interference from side lobes, enhancing overall network performance. The ability to create compact and highly efficient antennas makes it feasible to integrate them into a wide range of devices, including smartphones, IoT devices, and wearable technology. This facilitates more seamless integration of 5G capabilities into everyday technology. Therefore, the proposed antenna arrays can be used for 5G wireless communication systems.

References

[1] Gemeda, Mulugeta T., and Kinde A. Fante. "Inset-Feed Rectangular Microstrip Patch Antenna Array Performance Enhancement for 5G Mobile Applications." *In International Conference on Advances of Science and Technology*, pp. 284-303. Springer, Cham, 2020.

[2] Ayane L. Goshu, Mulugeta T. Gemeda and Kinde A. Fante — (2022). "Planar Microstrip Patch Antenna Arrays with Semi-elliptical Slotted Patch and ground Structure for 5G Broadband Communication Systems." *Cogent Engineering*, 9:1, 2069069, DOI: 10.1080/23311916.2022.2069069.

[3] Abubar, Abd Rahman, Mutiara Widasari Sitopu, Panangian Mahadi Sihombing, Jhoni Hidayat, and Afandi Sahputra. "Microstrip Antenna Design with Left Handed Metamaterial (LHM) for Automatic Dependent SurveillanceBroadcast (ADS-B)." *In 2020 4th International Conference on Electrical, Telecommunication and Computer Engineering (ELTICOM)*, pp. 103- 106. IEEE, 2020.

[4] D. Pattar, P. Dongaokar, and N. S L, "Metamaterial for design of compact microstrip patch antenna," *2020 IEEE Bangalore Humanitarian Technology Conference (B-HTC)*, 2020.

[5] Reena, Parihar. "A Compact Metamaterial inspired Dual-band SRR loaded Antenna for Wireless Applications." *Research Journal of Quantum Computations and Physical Systems*, Vol 1 (2018): 1.

[6] P. D. Tung, P. H. Lam, and N. T. Quynh Hoa, "A miniaturization of microstrip antenna using negative permittivity metamaterial based on CSRR-loaded GROUNDFOR WLAN applications," *Vietnam Journal of Science and Technology*, vol. 54, no. 6, p. 689, 2016.

[7] M. LABIDI and F. CHOUBANI, "A design of metamaterials MIMO antenna for Millimeter Wave Application," *2019 International Conference on Software, Telecommunications and Computer Networks (SoftCOM), 2019*.

[8] R. Goyal and Y. K. Jain, "Metamaterial based microstrip patch antenna using unit cell array for gain enhancement," *International Journal of Computer Sciences and Engineering*, vol. 7, no. 4, pp. 285–288, 2019.

[9] Baena, J. D., A. C. Escobar, A. Sayanskiy, and S. B. Glybovski. "Lefthanded metamaterials matched to free space through mechanical tuning." *In 2019 Thirteenth international congress on artificial materials for novel wave phenomena (Metamaterials)*, pp. X-044. IEEE, 2019.

[10] Jairath, Kapil, Navdeep Singh, Vishal Jagota, and Mohammad Shabaz. "Compact ultrawide band metamaterialinspired split ring resonator structure loaded band notched antenna." *Mathematical Problems in Engineering*, 2021.

[11] Esmail, B. A. F., H. A. Majid, F. A. Saparudin, M. Jusoh, A. Y. Ashyap, Najib Al-Fadhali, and M. K. A. Rahim. "Negative refraction metamaterial with low loss property at millimeter wave spectrum." *Bulletin of Electrical Engineering and Informatics 9*, no. 3 (2020): 1038-1045.

[12] A. Islam, E. Emon, and A. Ahmed, "A metamaterial loaded microstrip patch antenna for Lower 5G U-NII Spectrum," *Mathematical Modelling of Engineering Problems*, vol. 7, no. 4, pp. 556–562, 2020.

[13] A. A. Bakr Binshitwan, S. Mohamed Keskeso, A. A. Alquzayzi, and A. Elbarsha, "38GHz rectangular microstrip antenna with DGS for 5G applications," *2021 International Congress of Advanced Technology and Engineering (ICOTEN)*, 2021.

[14] H. Marzouk, A. Shaalan, and M. Ahmed, "A two-element microstrip antenna 28/38 GHz for 5G mobile applications," *Delta University Scientific Journal*, vol. 3, no. 1, pp. 1–8, 2020.

[15] B. Chauhan, S. Vijay, and S. C. Gupta, "Millimeter-wave mobile communications microstrip antenna for 5G a future antenna," *International Journal of Computer Applications*, vol. 99, no. 19, pp. 15–18, 2014.

[16] E. I. Hassan, R. I. Hamad, and M. I. Omar, "A 38 GHz modified circular microstrip patch antenna for 5G Mobile Systems," *2021 38th National Radio Science Conference (NRSC)*, 2021.

[17] Mohamad Aizwan Bin, Sulaim Bin Ab Qais, "Design of a Rectangular patch Microstrip Patch Antenna for 5G Applications." *University of Technology of Marash Alam Malaysia*.

[18] Rafique, Umair, Shobit Agarwal, Hisham Khalil Nasir Nauman, and Khalil Ullah. "Inset-fed planar antenna array for dual-band 5G MIMO applications." *Progress In Electromagnetics Research C 112*, pp. 83-98, 2021.

[19] Samarth Agarwal and Prahi. "High Gain Linear 1x4 X-slotted Microstrip Patch Antenna Array for 5G Mobile Technology." *Model Institute of Engineering and Technology, Jammu, India*, 2020.

[20] Gemeda, M. T., Fante, K. A., Goshu, H. L., and Goshu, A. L. (2021). "Design and Analysis of a 28 GHz Microstrip Patch Antenna for 5G Communication Systems." *International Research Journal of Engineering and Technology (IRJET)*, 8(02), 881-886.

[21] Sandi, Efri, Rizqiana Putri, and Aodah Diamah. "A Proposed Model of Metamaterial Complementary Split-Ring Resonator to Reduce Microstrip Array Antenna Dimension." *KnE Social Sciences (2019)*: 565-572.

[22] Ren, Kun, Pengwen Zhu, Taotao Sun, Junchao Wang, Dawei Wang, Jun Liu, and Wensheng Zhao. "A Complementary Split-Ring Resonator (CSRR)-Based 2D Displacement Sensor." *Symmetry 14*, no. 6 (2022): 1116.

[23] Sandi, E., A. Diamah, M. W. Iqbal, and D. N. Fajriah. "Design of substrate integrated waveguide to improve antenna performances for 5G mobile communication application." In Journal of Physics: Conference Series, vol. 1402, no. 4, p. 044032. IOP Publishing, 2019.

[24] Sandi, E., A. Diamah, M. W. Iqbal, and D. N. Fajriah. "Design of substrate integrated waveguide to improve antenna performances for 5G mobile communication application." In Journal of Physics: Conference Series, vol. 1402, no.4, p. 044032. IOP Publishing, 2019.

Authors' Profiles

Moti Beyene Gole received his MSc degree in Electronics Communication Engineering from Jimma University in 2023. He also received B.Sc. degree in Electrical and Computer Engineering from Debrebirhan University, Ethiopia, in 2018. He worked as an instructor in Jimma Institute of Technology in the Faculty of Electrical and Computer Engineering, Jimma University until 2019. Currently he is an Electrical Engineer in Ethiopian Electric Utility, Ethiopia. His research interests include metamaterial antenna, cyber security, and neural network.

Isayiyas Nigatu Tiba earned his Ph.D. in Information and Communications Engineering from Xidian University, Xi'an, China, in 2021. His doctoral research focused on a design of massive MIMO detectors via deep learning, contributing significantly to the applications AI to the physical layer communication. He is currently an Assistant Professor of Electrical and Computer Engineering. Currently, he serves as an Assistant Professor of Electrical and Computer Engineering at the Jimma University Institute of Technology in Jimma, Ethiopia. In this role, Dr. Isayiyas is dedicated to advancing the field of electrical and computer engineering through innovative teaching methods and cutting-edge research. His areas of expertise include wireless communications, Signal Processing for Communication Systems, and applications of Deep Learning for Wireless Communications, and he is actively involved in 2 active projects.

How to cite this paper: Moti G. Beyene, Isayiyas T. Nigatu, "Metamaterial Inspired Millimeter-Wave Antenna Arrays for 5G Wireless Applications", International Journal of Wireless and Microwave Technologies(IJWMT), Vol.15, No.1, pp. 40-50, 2025. DOI:10.5815/ijwmt.2025.01.03